



ELSEVIER

Contents lists available at ScienceDirect

Physica B

journal homepage: www.elsevier.com/locate/physb

Characterization of nanocomposite polymer electrolyte based on P(ECH-EO)

H. Nithya^a, S. Selvasekarapandian^{a,b,c,*}, P. Christopher Selvin^d, D. Arun Kumar^{b,a},
M. Hema^a, D. Prakash^e

^a DRDO-BU Center for Life Sciences, Bharathiar University, Coimbatore, Tamil Nadu, India

^b Department of Physics, Bharathiar University, Coimbatore, Tamil Nadu, India

^c Kalasalingam University, Krishnankoil, Srivilliputhur-626 190, Tamil Nadu, India

^d Department of Physics, NGM College, Pollachi, Tamil Nadu, India

^e Department of Physics, Alagappa University, Karaikudi, Tamil Nadu, India

ARTICLE INFO

Article history:

Received 3 August 2010

Received in revised form

15 May 2011

Accepted 22 May 2011

Available online 1 June 2011

Keywords:

P(ECH-EO)

ZrO₂

Differential scanning calorimetry

Electrical properties

ABSTRACT

ZrO₂ nanoparticles have been prepared by poly acrylamide gel route. The synthesized nanosized ZrO₂ have been incorporated into plasticized polymer electrolyte (PPE), P(ECH-EO): LiClO₄: γ -BL system to understand the effect of ZrO₂ on the ionic conductivity. The X-ray diffraction pattern of the synthesized ZrO₂ nanoparticles reveals the crystalline phase. The X-ray diffraction patterns of P(ECH-EO) based NCPPEM confirm the polymer–salt–nanoparticle complexation. The scanning electron microscope image of NCPPEM confirms that the ZrO₂ nanoparticles were distributed uniformly in the polymer matrix. The presence of nano filler has increased the ionic conductivity and the maximum dc conductivity value is found to be $6.24 \times 10^{-6} \text{ S cm}^{-1}$ at 303 K for 96(PPE): 4ZrO₂ (mol%).

© 2011 Elsevier B.V. All rights reserved.

1. Introduction

The development of a new polymer electrolyte to be used in advanced batteries and fuel cell is critical for the commercial success of these types of power systems. The problems faced in using the polymer electrolyte as electrolyte material in batteries and fuel cells are their low ionic conductivity at ambient temperature, reaction with the lithium metal electrode, and mechanical stability for use as an electrolyte. A lot of research efforts have been made to optimize the properties of polymer electrolytes for its applicability in solid-state lithium polymer electrolyte battery [1–4]. In the past two decades, a number of polymer electrolytes based on poly (acrylonitrile) [5], poly (propylene oxide) [6] and polyethylene oxide (PEO) [7,8] etc. have been investigated to meet these requirements to some extent. Among all these polymers, the polyether, polyethylene oxide, remained as one of the most preferred polymer matrix, since it is the best matrix for the alkaline salts [9,10]. Due to its high crystalline nature, PEO based electrolytes show high ionic conductivity only above its melting temperature (65 °C), which is inadequate for most of the practical applications. In order to improve the electrical properties of PEO, it is necessary to modify the polymer structure to obtain a larger

proportion of the amorphous phase. Several strategies were used to decrease the crystalline nature of PEO and improve the conductivity of its complexes at room temperature. One way to generate this modification could be to use a substituted monomer in order to form another polymer, a copolymer or a terpolymer. Works on copolymers based on PEO have been reported to reduce the crystalline nature of PEO and to increase its ionic conductivity. Among the copolymers reported, the halogenated polyether, poly(epichlorohydrin co ethyleneoxide) (P(ECH-EO)), has been chosen as the host polymer to prepare the polymer electrolyte.

To enhance the ionic conductivity, several approaches have been made such as adding organic plasticizer, blending polymers, incorporating fillers, etc. The addition of plasticizer, though improves the conductivity of the polymer electrolyte, faces problems such as the electrolyte leakage which deteriorates the mechanical stability of the polymer electrolyte. This leads to serious problems in the battery application. The addition of inert filler into polymer matrix improves the mechanical stability, ionic conductivity and electrode electrolyte interfacial stability which are important factors affecting a battery [11–15]. Scrosati et al. [16] reported the effect of nanoparticles SiO₂, TiO₂ fillers on the electrode electrolyte interfacial stability. Ahmad et al. have studied the effect of ZnO, TiO₂ and Al₂O₃ fillers on the room temperature conductivity of PVC:LiClO₄ [17]. Ji et al. have developed PEO:LiClO₄-SiO₂ composite electrolyte with improved conductivity in the order of $10^{-5} \text{ S cm}^{-1}$ at ambient temperature [18]. Pitawala et al. have studied the effect of incorporation of

* Corresponding author. Kalasalingam University, Krishnankoil,

Srivilliputhur-626 190.

E-mail address: sekarapandian@yahoo.com (S. Selvasekarapandian).

Al₂O₃ filler along with the plasticizers EC and PC into the (PEO)₉:LiTf solid polymer electrolyte system. The incorporation of filler leads to a significant improvement in the ionic conductivity to an order of 10⁻⁴ S cm⁻¹ at 25 °C [19]. Hence, in the present study nano sized ZrO₂ have been synthesized by the polyacrylamide gel method. The prepared nano sized ZrO₂ have been used for the preparation of nano composite polymer electrolyte membrane (NCPem) based on P(ECH-EO): γ -BL:LiClO₄ by the simple solution casting technique. XRD, SEM and conductivity studies have been used to study the effect of nanoparticles on the polymer electrolyte system P(ECH-EO): γ -BL:LiClO₄.

2. Experimental method

2.1. Synthesis of ZrO₂ nanoparticle

Monomers of acrylamide, (AM) and N-N'-methylene bisacrylamide (MBAM), were added to the aqueous solution of zirconium oxynitrate in the molar ratio 1:1. The initiators, ammonium persulfate (APS) and N,N,N',N'-tetramethyl ethylenediamide (TEMED) were then added to the transparent solution to initiate the free radical cross-linking polymerization between the AM and MBAM [20]. The transparent gel was obtained rapidly. The gel was then ground to get a homogeneous mixture and calcined at 600 °C for 6 h. The phase purity and the degree of the crystalline nature of the obtained ZrO₂ were studied by XRD analysis.

2.2. Preparation of nanocomposite polymer electrolyte membrane

The host polymer P(ECH-EO)(64%–36%)(Aldrich) and ionic dopant, lithium perchlorate (Himedia), were dried in vacuum, γ -butyrolactone (Merck) and acetone (Merck) were used as purchased. The nanocomposite polymer electrolyte membranes of various compositions were prepared by the simple solution casting technique as given below.

Based on the conductivity and the mechanical stability of the film, the ratio of plasticized polymer electrolyte, P(ECH-EO): γ -BL:LiClO₄ was kept fixed as 77.5:7.5:15. The plasticized polymer electrolyte 77.5 P(ECH-EO):7.5 γ -BL:15LiClO₄ (mol%) was considered as PPE. The homogeneous solution of P(ECH-EO): γ -BL:LiClO₄ was prepared by using acetone as solvent, to which ZrO₂ nanoparticle was dispersed and sonicated. The obtained colloidal solution was cast in the glass petri dishes and dried in vacuum oven at 50 °C to remove traces of acetone. The obtained thin film polymer electrolyte obtained after the removal of acetone was stored inside dessicator to avoid absorption of moisture. The different compositions of nanocomposite polymer electrolyte membrane prepared are,

Nanocomposite polymer electrolyte membrane (mol%)	Sample code
98(PPE): 2ZrO ₂	I1
96(PPE): 4ZrO ₂	I2
94(PPE): 6ZrO ₂	I3

The XRD diffractograms were recorded using PANanalytical X-pert pro-X-ray diffractometer using CuK α radiation. The SEM images were recorded using HITACHI S-3000 H scanning electron microscope. The thermal analysis has been carried out using Perkin Elmer STA6000 and NETZSCH DSC 204 F1. The electrical measurements have been carried out using computer controlled HIOKI 3532 LCZ analyzer in the frequency range of 42 Hz–1 MHz.

3. Results and discussion

3.1. Thermal analysis of ZrO₂

The TG/DTA traces of the polyacrylamide gel based ZrO₂ is presented in Fig. 1. The degradation of polymer gel takes place in multiple steps which completes around 600 °C. The weight loss of about 20% below 250 °C was attributed to the removal of the bound moisture. The elimination of the organic moieties through oxidation is observed by the weight loss step around 350 and 550 °C. The presence of nitrate ions initiates the degradation of polymeric network which is supported by the presence of exothermic peak around 250 °C in the DTA signal [21]. The gel completely decomposes at 600 °C which confirms the formation of ZrO₂.

3.2. Structural analysis of ZrO₂

< empty > X-ray diffraction studies have been employed to study the phase pure formation of ZrO₂. The XRD pattern of the

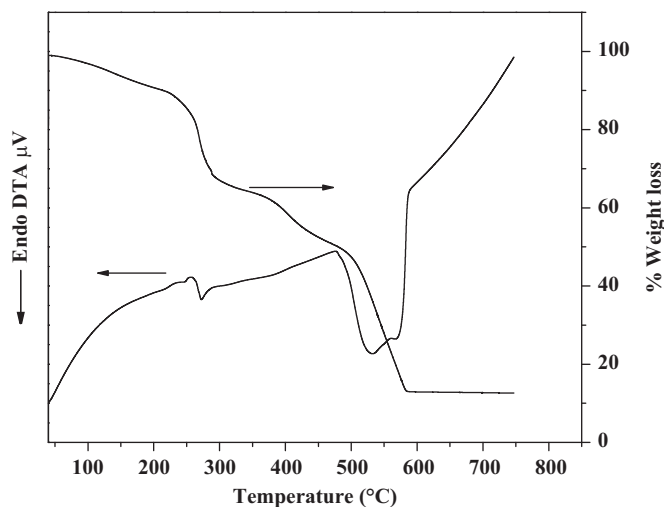


Fig. 1. TG/DTA curve ZrO₂ xerogel.

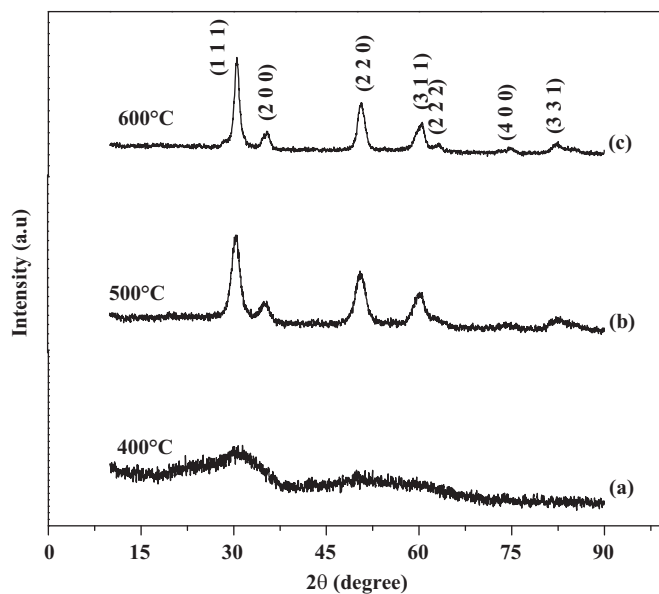


Fig. 2. XRD pattern of the synthesized ZrO₂ calcined at (a) 400 °C, (b) 500 °C and (c) 600 °C.

ZrO₂ calcined at 400, 500 and 600 °C is shown in Fig. 2(a–c). The ZrO₂ powder calcined at 400 °C shows the amorphous nature of the prepared powder indicating the presence of organic residues. The precursor calcined at 500 °C (Fig. 2(a–b)) shows the presence of ZrO₂ peaks with low crystallinity. The XRD pattern (Fig. 2(c)) shows a well resolved peak for the sample calcined at 600 °C, indicating the formation of phase pure ZrO₂ with high crystallinity. The result is compatible with the total weight loss results obtained from the TG/DTA analysis as shown in Fig. 1. The XRD pattern of ZrO₂ calcined at 600 °C shows intense peaks at 2θ values 30°, 35°, 50°, 60°, 74° and 82° corresponds to the (1 1 1), (2 0 0), (2 2 0), (3 1 1), (4 0 0) and (3 1 1) plane reflections respectively, which confirms the formation of single phase cubic structure of ZrO₂ [20–22]. The XRD pattern matches with JCPDS card no. 89-9069. The particle size was calculated using Debye–Scherrer formula

$$D = \frac{K\lambda}{\beta \cos\theta} \quad (1)$$

where, D represents the crystallite size, $K=0.94$, λ represents the wavelength of CuK α radiation and β represents the full width at half maxima of the diffraction peak.

The synthesized zirconia nanocrystallites were found to have an average particle size of 9 nm.

3.3. XRD analysis of NCPPEM

Fig. 3(a–e) shows the XRD pattern of LiClO₄, pure P(ECH-EO), P(ECH-EO)-LiClO₄ based nanocomposite polymer electrolyte. The complexation of ZrO₂ with the polymer electrolyte has been confirmed from the XRD pattern of the polymer complexes. In order to investigate the influence of ZrO₂ nanoparticle, XRD studies were performed for pure P(ECH-EO) and 98(PPE): 2ZrO₂ (mol%), 96(PPE): 4ZrO₂ (mol%), 94(PPE): 6ZrO₂ (mol%) nanocomposite polymer electrolyte. The following distinct features have been observed:

1. Fig. 3(a) shows intense peaks of angles $2\theta=21^\circ$, 23° , 27° , 31° and 35° which reveals the crystalline nature of ionic salt [JCPDS: 30-0751]. A broad peak at angle $2\theta=21^\circ$ in Fig. 3(b) reveals the amorphous nature of P(ECH-EO).
2. The peaks corresponding to LiClO₄ were not observed in Fig. 3(c–d) indicating that the LiClO₄ does not remain as a

separate phase in the polymer electrolyte system which confirms the complete dissociation of LiClO₄ in the polymer matrix.

3. The broadness of the peak at $2\theta=21^\circ$ shown in Fig. 3(c–d) increases with the addition of nano-sized ZrO₂ to the polymer electrolyte and the high intensity peaks of ZrO₂ are found to decrease. This suggests that the complexation of ZrO₂ with the polymer electrolyte takes place in the amorphous phase of the polymer to promote the local structural relaxation and segmental motion of the polymer. The peak angle at $2\theta=30^\circ$ corresponding to the ZrO₂ appears with increase in ZrO₂ concentration (Fig. 3(e)), which may be due to phase separation of ZrO₂ from the host polymer matrix at higher concentration of ZrO₂(6 mol%).

3.4. Morphological characteristics of NCPPEM

Fig. 4 shows the SEM image of the 96(PPE): 4ZrO₂ (mol%) nanocomposite polymer electrolyte membrane. It can be seen that the ZrO₂ nanoparticles are uniformly distributed in the polymer matrix. The presence of pores between the polymer interface and filler suggests that the plasticizer γ -BL is present both in the pores and P(ECH-EO) matrix. This paves way for the ionic conduction through the polymer matrix, ZrO₂ and the plasticizer [23].

3.5. Thermal analysis of NCPPEM

Thermal analysis has been performed using differential scanning calorimetric analysis in order to observe the change in glass transition temperature that is caused by the addition of ZrO₂. The DSC thermograms of pure polymer P(ECH-EO) and the nanocomposite polymer electrolyte are represented in Fig. 5. The DSC thermogram reveals an increase in glass transition temperature (T_g) with the addition of ZrO₂. The T_g of the pure P(ECH-EO) appears at 231 K. With the addition of ZrO₂, the T_g is increased to 239 K for 96(PPE): 4ZrO₂ (mol%). The increase in T_g with the addition of ZrO₂ may be due to the formation of ‘transient crosslinking’ between the oxygen ions in the polymer matrix and the Li⁺ ions which causes strong ion–dipole interactions in the polymer promoting a stiffening effect in the polymer

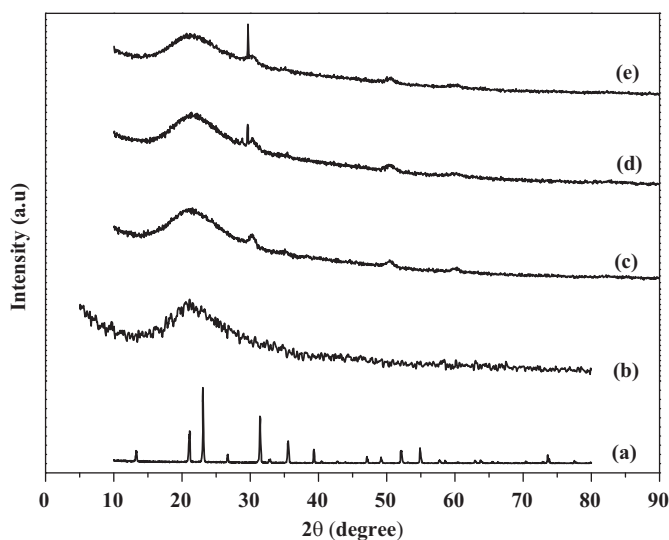


Fig. 3. XRD pattern of (a) LiClO₄, (b) pure P(ECH-EO), (c) 98(PPE): 2ZrO₂ (mol%), (d) 96(PPE): 4ZrO₂ (mol%) and (e) 94(PPE): 6ZrO₂.

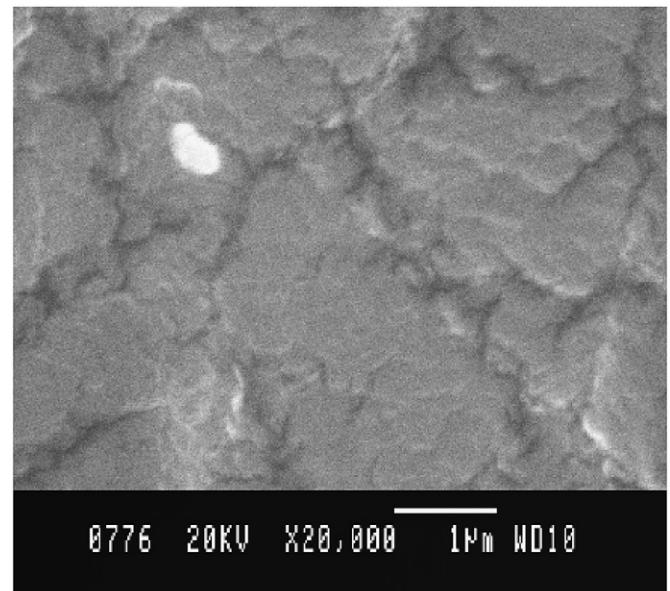


Fig. 4. SEM image of 96(PPE): 4ZrO₂ (mol%) nano composite polymer electrolyte membrane.

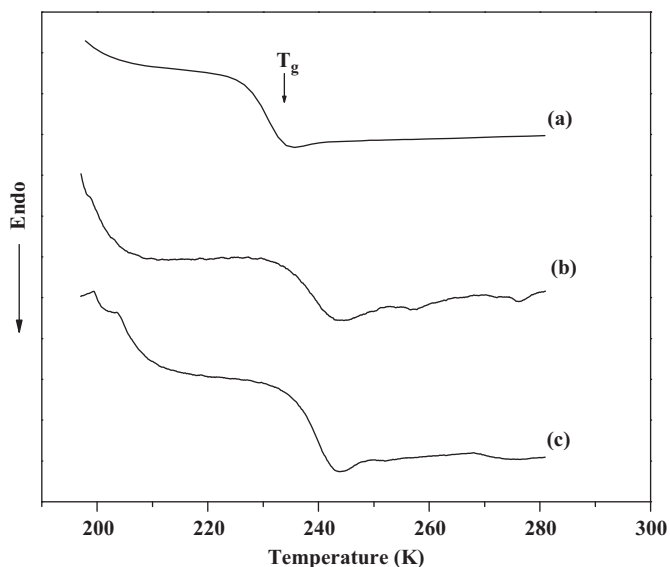


Fig. 5. DSC plot for (a) P(ECH-EO), (b) 98(PPE): 2ZrO₂ (mol%) and (c) 96(PPE): 4ZrO₂ (mol%).

chain [24]. Zoppi et al. [25] has reported similar effect for P(ECH-EO)/LiClO₄/SiO₂ polymer electrolyte.

3.6. Impedance spectroscopy analysis of NCPPEM

The complex impedance plot (Z' vs. Z'') for different compositions of the nano composite polymer electrolyte at 303 K is shown in Fig. 6a. The plot shows two well-defined regions, a high frequency semicircle and the low frequency spike. The high-frequency semicircle is related to bulk conduction processes [26]. The low-frequency spike results from electrode/electrolyte interface properties. Z-view software program was used to extract the bulk electrical resistance (R_b) of the polymer electrolytes. The bulk resistance values have been calculated from the low-frequency intercept on the real axis (Z') of impedance plot. The high-frequency semicircle is represented by the frequency dependent capacitor (C_g) parallel to the bulk resistance (R_b) and the low-frequency spike is represented by the constant phase element (CPE). The equivalent circuit is shown in Fig. 6b. The ionic conductivity is calculated using the relation

$$\sigma = l/(AR_b) \quad (2)$$

where A is the effective contact area of the sample with the electrode, R_b is the bulk resistance of the sample and l is the thickness of the sample.

From the impedance spectra, it is observed that the highest conductivity is found to be $6.24 \times 10^{-6} \text{ S cm}^{-1}$ at 303 K for the polymer electrolyte system with 4 mol% ZrO₂.

From the DSC results, it is observed that the glass transition temperature increases as the ZrO₂ concentration is increased. From the impedance spectra results, the ionic conductivity is found to increase with the increase in ZrO₂ concentration. In general, when the glass transition temperature increases, the ionic conductivity decreases. However, the experimental results obtained are contrary to this. From the investigation of the ionic conductivities of these nanocomposite polymer electrolytes, the samples show a conductivity enhancement. The only reason for the conductivity enhancement is the nanoparticles–polymer–plasticizer–salt interaction, especially the interaction of the nanoparticle's (ZrO₂) surface with the side chain of the polymer, but not much with the backbone of the main chain which has little effect on the mobility of Li⁺ ions at ambient temperature. Similar results have been

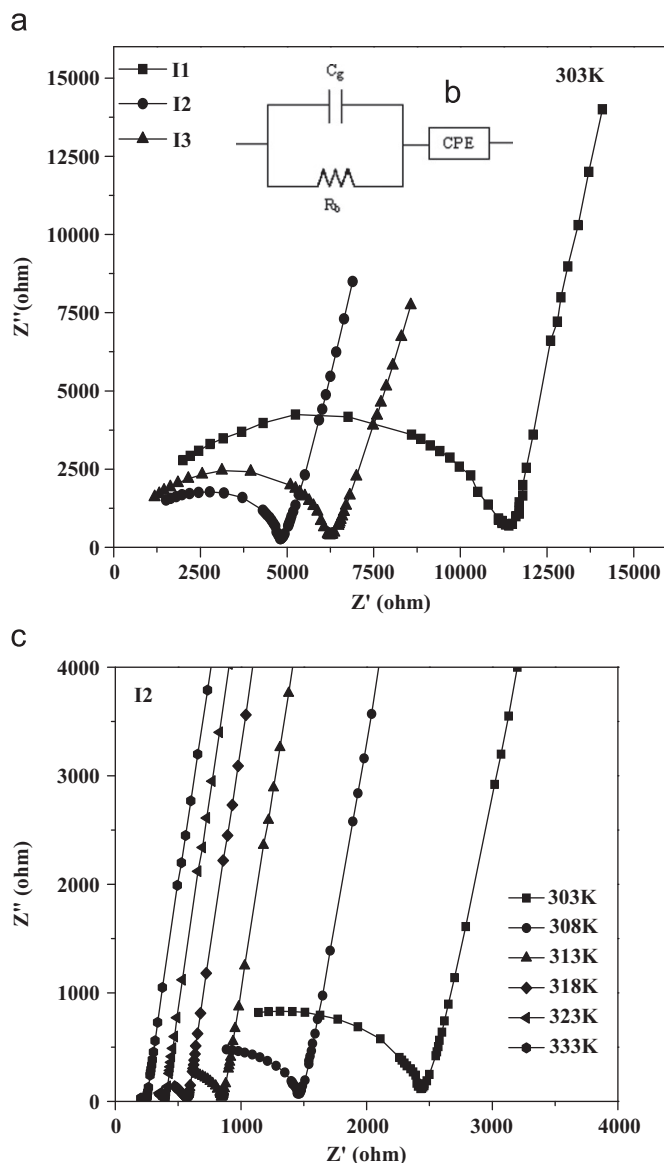


Fig. 6. Cole-Cole plot for (a) all composition at 303 K, (b) equivalent circuit: frequency independent capacitor C_g , constant phase element CPE and bulk resistance R_b and (c) 96(PPE): 4ZrO₂ (mol%) at different temperatures.

reported by Feng Zhao et al. [13] for the nanocomposite polymer electrolyte system poly (styrene-co-maleic anhydride) as the backbone and poly (ethylene glycol) methyl ether as side chain/SiO₂/LiCF₃SO₃.

The complex impedance plot for the highest conductivity electrolyte system 96(PPE): 4ZrO₂ (mol%) (12) at various temperatures is shown in Fig. 6(c). The bulk resistance decreases with the increase in temperature. Decrease in impedance corresponds to the increase in charge carrier density. In the complex impedance plot, the disappearance of the high-frequency semicircle with the increase in temperature reveals the absence of capacitive nature due to the random orientation of dipoles in the side chains of the polymer electrolyte [27]. Hence, it is found that the amount of ZrO₂ considerably increases the ionic conductivity of the nano composite polymer electrolyte.

3.7. Conductivity analysis of NCPPEM

The frequency dependence of conductivity for the entire polymer electrolyte at 303 K is shown in Fig. 7(a). The spectra

shows three well-defined regions: a low-frequency region, mid-frequency plateau region and the high-frequency dispersion region. The conductivity is found to obey Jonscher's power law [28]

$$\sigma(\omega) = \sigma_{dc} + A\omega^n \tag{3}$$

where σ_{dc} is the dc ionic conductivity, A and n are temperature dependent parameters. The dc conductivity values have been calculated by fitting the Jonscher's power law equation to the experimental data obtained and it is found that the values lie in the 10^{-6} S cm⁻¹ range at 303 K (Table 1) for all the composition. Fig. 7(b) shows the frequency dependent conductivity spectra of 96(PPE): 4ZrO₂ (mol%) (I2) the polymer electrolyte with high conductivity. At high temperatures, the low frequency spike is

observed which is due to the electrode polarization effects. At these temperatures the ionic conductivity is high due to the significant build-up of charges at the electrodes which reduces the effective applied field across the samples and apparently increases the ionic conductivity. The ionic conductivity increases from 10^{-6} to 10^{-4} Scm⁻¹ and the values are tabulated in Table 1. It is observed from the table that the conductivity reaches a maximum of 1.21×10^{-4} Scm⁻¹ at 333 K for nano composite polymer electrolyte system with 4 mol% ZrO₂. Also, at higher concentration of ZrO₂ (6 mol%), the conductivity decreases which may be due to the agglomeration of the inorganic particles (ZrO₂). The increase in conductivity with temperature is interpreted as the hopping of ions between the coordinating sites, local structural relaxations and segmental motion of the polymer matrix [29,30]. From the spectra it is clear that as the temperature is increased the spike gets increased due to the increase in mobile charge carrier and the DC plateau region shifts towards the high-frequency region. The high-frequency spike disappears as the temperature increases within the frequency region measured.

3.8. Temperature dependence of the ionic conductivity

The temperature dependent ionic conductivity of the composite polymer electrolytes was evaluated to analyze the mechanism of ionic conduction in polymer electrolyte. Fig. 8 shows the variation of ionic conductivity with the reciprocal of temperature for the nano composite polymer electrolytes. The linear variation of $\log \sigma$ versus $1000/T$ plots suggests an Arrhenius type thermally activated process. This suggests that there is no phase transition of nanocomposite polymer matrix in the temperature range studied. It is also supported by the results of the obtained DSC thermograms in this temperature range studied. The conductivity

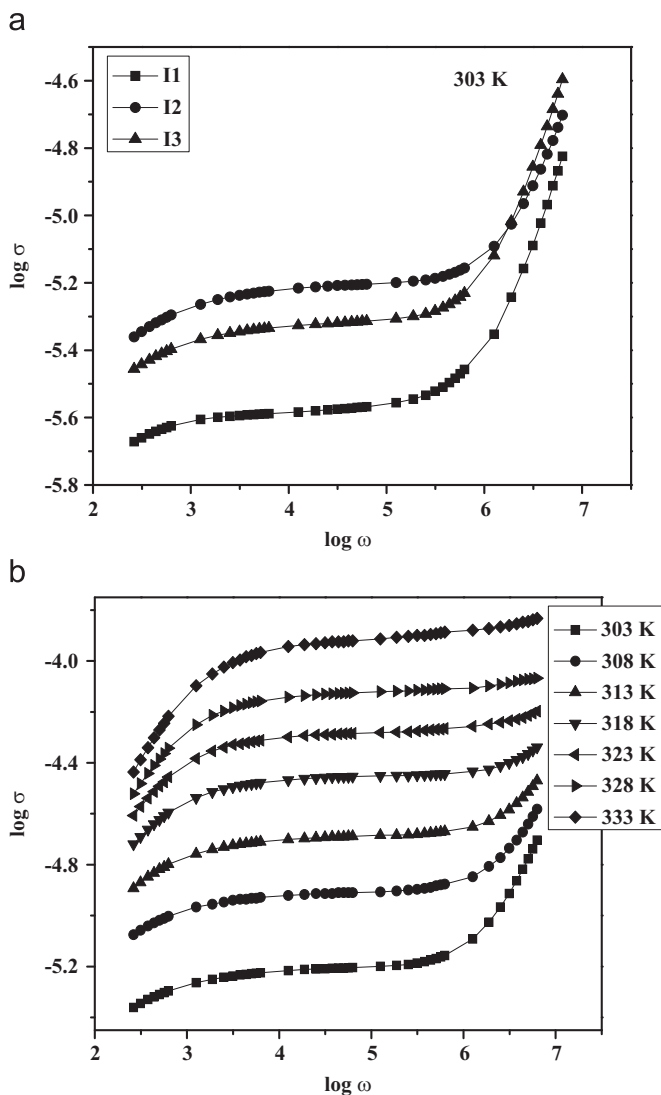


Fig. 7. Conductance plot of 96(PPE): 4ZrO₂ (mol%) at different temperatures.

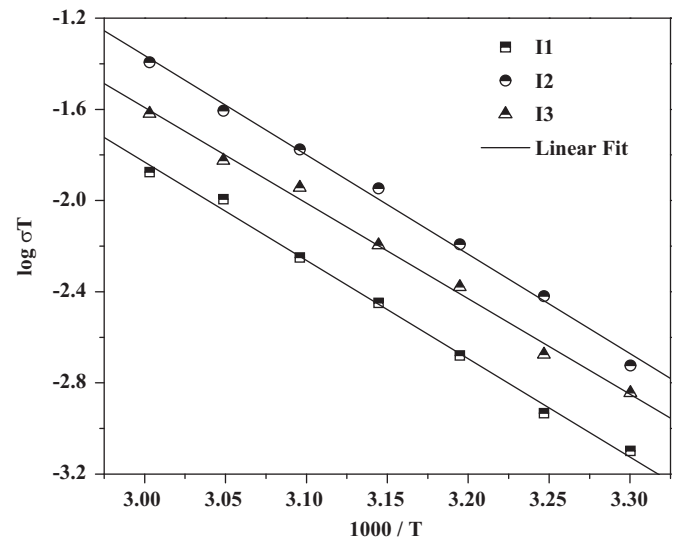


Fig. 8. Arrhenius plot for P(ECH-EO) based nanocomposite polymer electrolyte.

Table 1
Conductivity of the NCPem at different temperatures.

Nanocomposite polymer electrolyte membrane	Conductivity Scm ⁻¹			Activation energy (eV)
	303 K	318 K	333 K	
75.95P(ECH-EO):7.35 γ-BL:14.7LiClO ₄ : 2ZrO ₂ (I1)	2.62×10^{-6}	1.12×10^{-5}	4.00×10^{-5}	0.39
74.4P(ECH-EO):7.2 γ-BL:14.4LiClO ₄ : 4ZrO ₂ (I2)	6.24×10^{-6}	3.55×10^{-5}	1.21×10^{-4}	0.36
72.85P(ECH-EO):7.05 γ-BL:14.1LiClO ₄ : 6ZrO ₂ (I3)	4.32×10^{-6}	1.89×10^{-5}	7.05×10^{-5}	0.38

can be expressed as

$$\sigma_{dc} = \sigma_0 \exp(-E_a/KT) \quad (4)$$

where σ_0 is the pre-exponential factor, E_a is the activation energy and T is the absolute temperature in K . The activation energy values have been calculated from the slope of the Arrhenius plot. Table 1 shows the activation energy of nano composite polymer films with different compositions and the results reveal that E_a decreases effectively with the ZrO_2 concentration. As temperature increases, the polymer chain acquires faster internal modes in which bond rotations produce segmental motion. This, in turn, favours inter-chain hopping and intra-chain ion movements and, accordingly, the conductivity of the polymer electrolyte becomes high [31].

3.9. Dielectric behavior

The dielectric behavior of the highest conductivity nanocomposite polymer electrolyte membrane 96(PPE): 4ZrO₂ (mol%) (I2) is described by using the dielectric function ϵ^*

$$\epsilon^* = \epsilon' - i\epsilon'' \quad (5)$$

where ϵ' is dielectric constant and ϵ'' is dielectric loss

Fig. 9 shows $\log f$ vs. ϵ' plot at different temperatures for 96(PPE): 4ZrO₂ (mol%) (I2) polymer electrolyte. It is observed that the dielectric constant decreases with increasing frequency. A rapid decrease in dielectric constant may be noticed over the frequency range of 1 kHz. The decrease in the dielectric constant with the increase in the frequency may be due to the tendency of the dipoles in the polymer chains to orient themselves in the direction of the applied electric field [32]. The higher values of ϵ' for 96(PPE): 4ZrO₂ (mol%) at low frequency for the system is due to the enhanced charge carrier density at the electrolyte-electrode interface, resulting in an increase in the equivalent capacitance [33–35]. The observed variation in ϵ' with frequency can be attributed to the formation of space charge region at the electrode-electrolyte interface which is known as $\omega^{(n-1)}$ variation or the non-debye behavior where the space charge with respect to frequency is explained in terms of ion diffusion [36]. At high frequencies, the fast periodic reversal of the electric field occurs. Hence, the polarization due to charge accumulation decreases at the electrode-electrolyte interface which, in turn, contributes to the decrease in ϵ' [37].

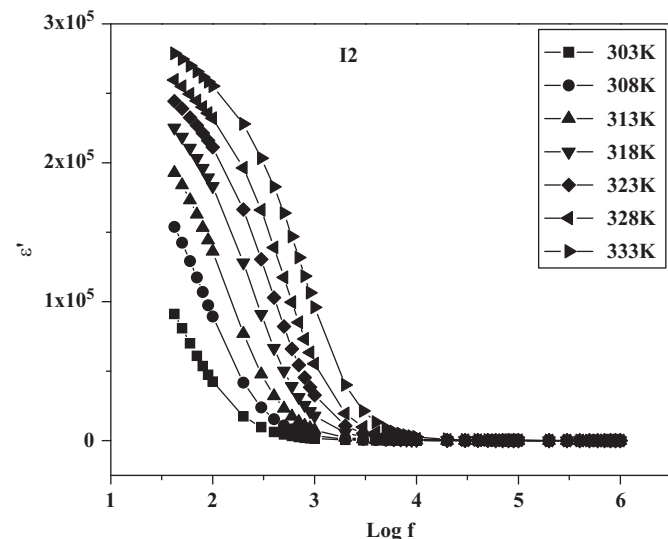


Fig. 9. Dielectric constant plot of 96(PPE): 4ZrO₂ (mol%) at different temperatures.

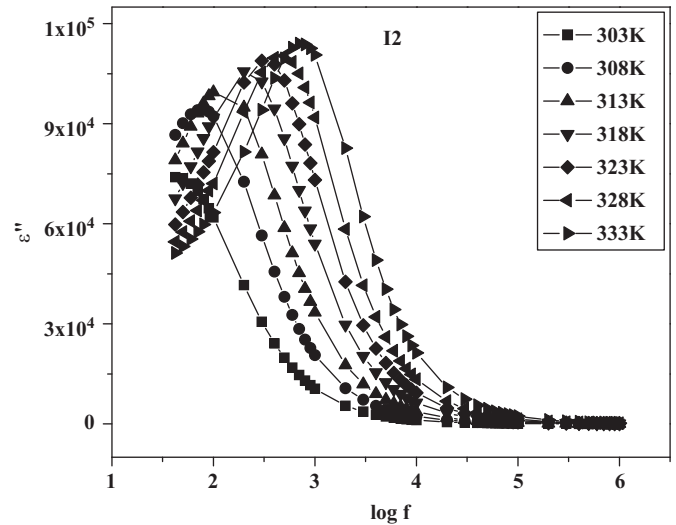


Fig. 10. Dielectric loss plot of 96(PPE): 4ZrO₂ (mol%) at different temperatures.

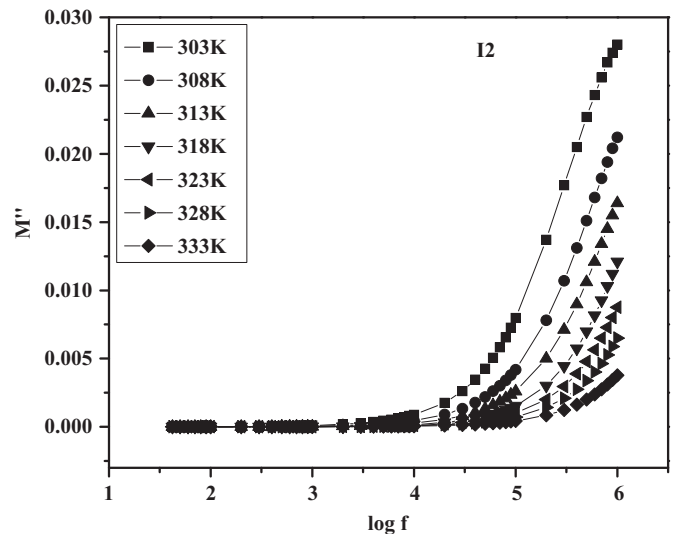


Fig. 11. Modulus plot of 96(PPE): 4ZrO₂ (mol%) at different temperatures.

Dielectric loss factor (ϵ'') is a direct measure of energy dissipated and is generally composed of the contributions from the ionic transport and from the polarization of the charge or dipole. Fig. 10 shows ϵ'' as a function of frequency in wide temperature range for 96(PPE): 4ZrO₂ (mol%) (I2). A decrease in dielectric loss at lower frequency and maximum in the mid-frequency have been observed in the 96(PPE): 4ZrO₂ (mol%) polymer electrolyte system. This observed peak is due to the β -relaxation which may be due to the movement of the side chains of the polymer. The shifting of β -relaxation to the high-frequency range with the increase in temperature indicates a decrease in the relaxation time of the side chains [38,39].

3.10. Electric modulus analysis

The dielectric behavior of the sample can also be studied using the electric modulus. Fig. 11 shows the frequency dependence of the imaginary part of the modulus for 96(PPE): 4ZrO₂ (mol%) (I2) nanocomposite polymer electrolyte membrane. It is observed that the modulus increases with the increase in frequency. At low frequency, the modulus value approaches to zero indicating that the electrode polarization phenomenon makes a negligible

contribution. The appearance of long tail in the low frequency region is due to the capacitance effect at the electrodes. The increases in modulus spectra at higher frequencies indicates that the polymer electrolyte systems are ionic conductors and this is attributed to the bulk of the material. The maximum of the peak decreases with the increase in temperature indicates distribution of relaxation mechanism [40].

4. Conclusion

The nanocomposite polymer electrolyte based on P(ECH-EO) has been prepared by the simple solution casting technique. The amorphous nature and the complexation of ZrO₂ to the polymer matrix have been confirmed by the XRD analysis. The uniform distribution of ZrO₂ in the polymer matrix has been analyzed by SEM. The nanocomposite polymer electrolyte membrane having 4 mol% ZrO₂ exhibits a maximum conductivity of $6.24 \times 10^{-6} \text{ Scm}^{-1}$ at 303 K. The dielectric spectra reveal β -relaxation process in the polymer electrolyte.

Acknowledgement

One of the authors, Ms. H. Nithya, would like to thank the DRDO-BU Center for Life Sciences for providing Senior Research Fellowship. The authors would like to thank Prof. T. Kurian Mathew (Retd.), Department of English, Devanga Arts College, Aruppukotai, Tamil Nadu, India for editing the manuscript for language.

References

- [1] Z. Gadjourova, Y.G. Andreev, D.P. Tunstall, P.G. Bruce, *Nature (London)* 412 (2001) 520.
- [2] P.A.R.D. Jayathilaka, M.A.K.L. Dissanayake, I. Albinsson, B.E. Mellander, *Electrochim. Acta* 47 (2002) 3257.
- [3] Y. Aihara, J. Kuratomi, T. Bando, T. Iguchi, H. Yoshida, T. Ono, K. Kuwana, *J. Power Sources* 114 (2003) 96.
- [4] Guoxin Jiang, Seiji Maeda, Huabin Yang, Yoichiro Saito, Shigeo Tanase, Tetsuo Sakai, *J. Power Sources* 141 (2005) 143.
- [5] H.S. Choe, B.G. Carroll, D.M. Pasquariello, K.M. Abraham, *Chem. Mater.* 9 (1997) 369.
- [6] C. Vachon, C. Labreche, A. Vallee, S. Benser, M. Dumont, J. Prud'homme, *Macromolecules* 28 (1995) 5585.
- [7] F.M. Gray, J.A. Connor (Eds.), *Polymer Electrolytes*, The Royal Society of Chemistry, Canterbury, UK, 1997.
- [8] F. Croce, L. Persi, B. Scrosati, F. Serraino-Fiory, E. Plichta, M.A. Hendrickson, *Electrochim. Acta* 46 (2001) 2457.
- [9] M.B. Armand, J.M. Chabagno, M.J. Duclot, in: P. Vashisha, J.N. Mundy, G.K. Shenoy (Eds.), *Fast ion transport in solids*, North Holland, Amsterdam, 1979 131.
- [10] D.F. Shriver, B.L. Papke, M.A. Ratner, R. Dupon., T. Wong, M. Brodwin, *Solid State Ionics* 5 (1981) 83.
- [11] H.M.J.C. Pitawala, M.A.K.L. Dissanayake, V.A. Seneviratne, *Solid State Ionics* 178 (2007) 885.
- [12] Xiangming He, Qiao Shi, Xiao Zhou, Chunrong Wan, Changyin Jiang, *Electrochim. Acta* 51 (2005) 1069.
- [13] Feng Zhao, Mingkui Wang, Li Qi, Shaojun Dong, *J. Solid State Electrochem* 8 (2004) 283.
- [14] Hui Xie, Zhiyuan Tang, Zhong yan Li, Yanbing He, Yong Liu, Hong Wang, *J. Solid State Electrochem* 12 (2008) 1497.
- [15] Shahzada Ahmad, S.A. Agnihotry, *Curr. Appl. Phys.* 9 (2009) 108.
- [16] B. Scrosati, F. Croce, R. Curini, A. Martinello, L. Persi, F. Ronci, R. Caminiti, *J. Phys. Chem. B* 103 (1999) 10632.
- [17] A. Ahmad, M.Y.A. Rahman, M.S. Su'ait, *Phys. B: Condens. Matter* 403 (2008) 4128.
- [18] Kwang-Sun Ji, Hee-Soo Moon, Jong-Wook Kim, Jong-Wan Park, *J. Power Sources* 117 (2003) 124.
- [19] H.M.J.C. Pitawala, M.A.K.L. Dissanayake, V.A. Seneviratne, B.E. Mellander, I. Albinsson, *J. Solid State Electrochem.* 12 (2008) 783.
- [20] P.S. Sonawane, Santhoshkumar S. Biradar, S. Radhakrishnan, B.D. Kulkarni, *Mater. Chem. Phys.* 105 (2007) 348.
- [21] M. Tahmasebpour, A.A. Babaluo, M.K. Razavi Aghjeh, *J. Eur. Ceram. Soc.* 5 (28) (2008) 773.
- [22] Mahnaz Masoud Salavati-Niasari, Fatemeh Davar Dadkhah, *Inorg. Chim. Acta* 362 (2009) 3969.
- [23] N.T. Kalyana Sundaram, T. Vasudevan, A. Subramania, *J. Phys. Chem. Solids* 68 (2007) 264.
- [24] S. Kohjiya, Y. Matoba, K. Miura, M. Kitagawa, T. Sakashita, T. Horiuchi, Y. Ikeda, *Polym. Int.* 49 (2000) 197.
- [25] R.A. Zoppi, C.M.N.P. Fonseca, M.-A. De Paoli, S.P. Nunes, *Acta Polym.* 48 (1997) 193.
- [26] R.D. Armstrong, *J. Electroanal. Chem.* 52 (1974) 413.
- [27] R. Baskaran, S. Selvasekarapandian, N. Kuwata, J. Kawamura, T. Hattori, *Mater. Chem. Phys.* 98 (2006) 55.
- [28] A.K. Jonscher, *Nature* 267 (1977) 673.
- [29] R. Baskaran, S. Selvasekarapandian, N. Kuwata, J. Kawamura, T. Hattori, *Solid State Ionics* 177 (2006) 2679.
- [30] B. Kumar, S.J. Rodrigues, *J. Electrochem. Soc.* 148 (2001) A1336.
- [31] Ch.V. Subba Reddy, A.K. Sharma, V.V.R. Narasimha Rao, *J. Power Sources* 14 (2003) 338.
- [32] A.M.A. Nada, M. Dawy, A.H. Salama, *Mater. Chem. Phys.* 84 (2004) 205.
- [33] R. Mishra, K.J. Rao, *Solid State Ionics* 106 (1998) 113.
- [34] J.A. Campbell, A.A. Goodwin, G.P. Simon, *Polymer* 42 (2001) 4731.
- [35] F.S. Howell, R.A. Bose, P.B. Macedo, C.T. Moynithan, *J. Phys. Chem.* 78 (1974) 639.
- [36] J.R. Macdonald (Ed.), *Impedance Spectroscopy*, Wiley, New York, 1987.
- [37] S. Ramesh, A.H. Yahaya, A.K. Arof, *Solid State Ionics* 152–153 (2002) 291.
- [38] Otto van den Berg, Wolter F. Jager, Wilco G.F. Sengers, Michael Wubbenhorst, Stephen J. Picken, *Polym. Mater.: Sci. Eng.* 90 (2004) 1597.
- [39] Borisova, *Relaxation Phenomena in Polymers*, in: G.M. Bartnew, Y.V. Zelenew, Halsted (In Ed.) NewYork, 1974, 25.
- [40] S. Ramesh, Tai Fung Yuen, Chia Jun Shen, *Spectrochim. Acta, Part A* 69 (2008) 670.